

# Magnetic flares in accretion disc coronae and the Spectral States of black hole candidates: the case of GX 339-4.

T. Di Matteo <sup>1</sup>, A. Celotti <sup>1,2</sup> and A.C. Fabian <sup>1</sup>

<sup>1</sup>*Institute of Astronomy, Madingley Road, Cambridge, CB3 0HA*

<sup>2</sup>*S.I.S.S.A., via Beirut 2–4, 34014 Trieste, Italy*

20 August 2021

## ABSTRACT

We present a model for the different X-ray spectral states displayed by Galactic Black Hole Candidates (GBHC). We discuss the physical and spectral implications for a magnetically structured corona in which magnetic flares result from reconnection of flux tubes rising from the accretion disk by the magnetic buoyancy (Parker) instability. Using the observations of one of the best studied examples, GX339-4, we identify the geometry and the physical conditions characterizing each of these states. We find that, in the Soft state, flaring occurs at small scale heights above the accretion disk. The soft thermal-like spectrum, characteristic of this state, is the result of heating and consequent re-radiation of the hard X-rays produced by such flares. The hard tail is produced by Comptonization of the soft field radiation. Conversely, the hard state is the result of a phase in which flares are triggered high above the underlying accretion disk and produce X-rays via Comptonization of either internal cyclo-synchrotron radiation or of soft disk photons. The spectral characteristics of the different states are naturally accounted for by the choice of geometry: when flares are triggered high above the disk the system is photon-starved, hence the hard Comptonized spectrum of the hard state. Intense flaring close to the disk greatly enhanced the soft-photon field with the result that the spectrum softens. We interpret the two states as being related to two different phases of magnetic energy dissipation. In the Soft state, Parker instability in the disk favours the emergence of large numbers of relatively low magnetic field flux tubes. In the hard state, only intense magnetic fields become buoyant and magnetic loops are able to rise and expand in the coronal atmosphere. The model can also qualitatively account for the observed short timescale variability and the characteristics of the X-ray reflected component of the hard state.

**Key words:** radiation mechanisms - magnetic fields - galaxies: active - binaries: general - accretion discs

## 1 INTRODUCTION

Galactic X-ray sources are classified as black holes candidates (GBHC) if either the measured binary mass function indicates the presence of an object with  $M \gtrsim 3M_{\odot}$  (for a review see Tanaka & Lewin 1995) or their high energy X-ray spectra and temporal variability are similar to other GBHC.

For many years GBHC have been known to radiate in five different spectral states, defined by the observed spectral components and flux level typically in the 1 – 10 keV band. Systems in the *Hard/Low state* emit most of their energy in a hard tail which can be represented as a power law with a photon index  $\Gamma \sim 1.3 - 1.7$  and an exponential cut-off at about 100 keV (Tanaka & Lewin 1995, Zdziarski et al. 1997). Most of these objects are also observed in a

*Soft/High State*, when most of the energy is emitted in a blackbody component with characteristic temperature in the range of 0.6 – 1 keV. In addition to this thermal component the spectrum comprises a power law, characterized by a slope  $\Gamma = 2.0 - 2.5$ , which dominates above  $\sim$  few keV. It was originally thought that the GBHC systems were much more luminous in the soft than in the hard state, but recent observations of GX339-4 and Cyg X-1 have shown that despite their dramatic spectral changes the bolometric luminosity changes only slightly.

Although the hard and soft states are the most common ones, occasionally GBHC have been observed in three other states (these occur as transitional events and have been observed rather infrequently). The *Intermediate State* is seen during transitions between the low and high state. In the

*Very High State*, GBHC have the highest luminosity: the high-energy power law component has a flux comparable to the soft blackbody one and the high energy emission does not show any sign of a cut-off. In the *Off State*, spectra are completely dominated by a power-law ( $\Gamma = 1.7$ ) component with a flux level lower than in the hard state by a few orders of magnitude.

Another important signature of the different source behaviour in the different spectral states is the variability pattern. In the soft state the normalization of the power law has been observed to vary whereas the soft blackbody component is very stable. The emission in the hard state instead shows extreme variability on time scales as short as  $10^{-3}$  s. Short timescale variability is also observed in the power law of the very high state.

Although temporal and spectral behaviors of GBHC have been widely studied in the last few years, the nature of the different spectral states and in particular the mechanism driving the transition from one to the other are largely unknown. The thermal radiation, characteristic of the high, very high and intermediate states is generally modeled to be blackbody emission from a (standard) optically thick accretion disk. The power law component is generally attributed to inverse Compton radiation from an optically thin corona sandwiching the accretion disk. The presence of such a hot medium was initially hypothesized in the context of Seyfert galaxies (e.g. Haardt & Maraschi 1993) and because of the similarity between the spectra of Seyfert galaxies and those of GBHC in the hard state, the same model was naturally extended to the galactic objects too. In the Seyferts scenario it has also become necessary, in order to account for the different ratios of UV vs X-ray luminosity and the extremely short variability time scales observed, to assume that such a corona actually consists of localized active regions (e.g. Haardt, Maraschi & Ghisellini 1994, Stern et al. 1995, Nayakshin & Melia 1997a,b). Such regions could be the end result of impulsive magnetic energy dissipation (i.e. reconnection) in flux tubes emerging from the disk by buoyant instability (as originally suggested by Galeev, Rosner & Vaiana 1979).

In GBHC different geometries for the spatial distributions of the hot and cold matter associated with the accretion flow have been proposed. Some models (Dove et al. 1997, Gierlinsky et al. 1997, Poutanen, Krolik & Ryde 1997) deduce the geometry of the emitting regions from the spectral analysis of the different states. In particular, the authors of such models argue that because the reflection component in the hard state of GBHC is much less prominent than in Seyferts, the inner radius of the disk must be far away from the black hole, in order to subtend a small solid angle to the X-ray emitting region. Most of the energy would be dissipated in a thermally hot central cloud/corona-like structure which, by Comptonization, produces the observed spectrum. In the soft state the optically thick cool disk is postulated to move inwards and the majority of the dissipated energy would emerge in the form of a blackbody-like spectrum. In these scenarios, though, no physical mechanism is provided to explain the origin of such drastic changes in the geometry of the inner region between the two states. A possible interpretation has been discussed by Esin, McClintock and Narayan (1997) in the context of advection-dominated accretion flow (ADAF) solutions. In these models the inner

Compton cloud in the hard state is identified with an advection dominated zone (with still an outer thin disk at larger radii). As the accretion rate increases an ADAF is no longer allowed and it shrinks in size. The outer thin disk moves inwards and the spectrum changes from hard to soft. It should be noticed that although the geometry of the X-ray emitting region in both classes of models (the Compton cloud and the advection-dominated) predicts the observed lack of reflected emission, it can not explain the fast variability time scales observed in the hard states of GBHC.

In this paper we show that the different spectral components and the different spectral states of GBHC can be easily reproduced within the context of a magnetically structured corona by considering flares triggered at different scale heights above an accretion disk. We expect such a corona to form because the strong magnetic fields, continuously generated by the dynamo action in an accretion disk, are strongly buoyant and are forced to invade the region sandwiching the disk itself. Once outside the disk the magnetic flux tubes can reconnect efficiently and dissipate part of the accretion energy in localized active flares.

Here, we shall, at first, constrain the geometry and the energy dissipation distribution of the emitting regions in the different states exclusively from the detailed broad band spectral information provided by the observations. In Section 2 we will give an overview of our model, and specify the parameters which can be derived almost directly from observations and those related to the system geometry. In particular, we will consider the spectral implications of having localized active regions at different scale heights above the accretion disk. In section 4 we will obtain the parameter spaces which characterize the different spectral states by applying our model to GX339-4 (we summarize the data collected from the literature in section 3). In section 5 we will relate the properties of the active coronal regions derived from the physics of radiation, to those of a magnetically structured corona. We will show that our model is completely consistent with the idea that X-ray flares are the after effect of reconnection of magnetic flux tubes rising from the accretion disk due to magnetic buoyancy. The different spectral states can then be identified with different phases of flare activity. Such phases would, in turn, be regulated by the physical conditions in the accretion disk relevant for the onset of buoyancy instability. Finally, in Section 6 we briefly discuss our model predictions for the variability and the reflection properties in the different states.

## 2 THE MODEL

### 2.1 Emission from a magnetically structured corona

As already mentioned, we adopt a model for a magnetically structured accretion disk corona in which localized active regions (magnetic loops) form as a result of magnetic buoyancy instability in the underlying accretion disk. Buoyancy constitutes a mechanism that channels part of the energy released in the accretion process directly to the corona outside the disk. Therefore, following Di Matteo, Celotti & Fabian (1997), we assume that a significant fraction  $f$  of the accretion power,  $\eta L_{\text{Edd}}$ , is dissipated magnetically in the corona

while the remaining fraction  $(1 - f)$  is dissipated internally to the disk. The magnetic field strength  $B$  in the magnetic flux tubes is therefore given by

$$B = 9 \times 10^7 \left( \frac{f\eta}{N_{\text{tot}}} \right)^{1/2} r^{-1} \left( \frac{10 M_{\odot}}{M} \right)^{1/2} \text{ G}, \quad (1)$$

where  $N_{\text{tot}}$  is the number of magnetic loops emerging from the disk,  $L_{\text{Edd}}$  is the Eddington luminosity,  $r$  is their typical size in units of the Schwarzschild radius,  $R_s$ , and  $M$  is the black hole mass which we take  $M = 10 M_{\odot}$ . Although a number  $N_{\text{tot}}$  of magnetic loops become buoyant, there will only be a certain number  $N$  of loops reconnecting (i.e. producing flares) at any given time. We take  $N = 10$  as the number of active regions needed to explain (from simple Poissonian noise) X-ray fluctuations of a factor  $\sim 2$  on short timescales which are typically observed in GBHC.

Here we consider a situation in which the majority of the accretion power, say  $f \sim 80$  per cent, is released into the magnetic structures in the corona and only  $\sim 20$  per cent in the optically thick disk. Such an assumption implies that the X-ray emission from the active coronal regions plays a fundamental role in the production of the different spectral components observed in the various states of GBHC, as we shall show in the course of this section.

The hard X-ray emission is produced in the corona by thermal Comptonization of soft seed photons produced both as blackbody radiation in the underlying accretion disk and as cyclo-synchrotron by the same hot electrons pervading the corona. Cooling by cyclo-synchrotron emission and its relative Comptonization are not usually taken into account in disk-corona models, but they can be the dominant radiative processes in the GBHC scenario (Di Matteo et al. 1997).

The luminosity and the effective temperature of the quasi-thermal component emitted by the accretion disk are consistently estimated as due to both the intrinsic energy dissipation and to the re-radiation of the coronal hard X-rays impinging on and then being absorbed/reflected by the disk.

The relative importance of all of these different processes is mostly and critically dependent on the assumed geometry of the system. We therefore considered the predictions of this schematic model (more details are given below) against the observed spectral properties of one of the most well known GBHC, namely GX339-4, in order to: a) determine the dominant emission processes in the different spectral states; b) explore the role of the spatial and geometrical distributions of such active regions and set any possible constraint. As we shall see in the following sections, the observed spectral states strongly limit the geometrical (and consequently physical) characteristics of active regions.

### 2.1.1 Model parameters

The Comptonized (energy) spectrum is described by a power law of slope  $\alpha$  with an exponential cut-off at an energy  $E_C$ .  $\alpha$  is a function of both  $\tau$  and  $\theta$ , the Thomson optical depth of the scattering region and the dimensionless electron temperature ( $\theta = kT/m_e c^2$ ), respectively. This can be expressed as  $\alpha \simeq -\ln P / \ln(1 + 4\theta + 16\theta^2)$  where  $P$  is the average scattering probability  $P = 1 + \exp(-\tau)/2 (\tau^{-1} - 1) - 2\tau^{-1} + (\tau/2)E_1(\tau)$ , and  $E_1$  the exponential integral (Zdziarski et

al. 1994 – also consistent with the analytical approximation  $\alpha = 0.16/(\tau\theta)$  by Pietrini & Krolik 1995). Two more parameters describe the soft (disk) blackbody component, namely its effective temperature  $T_{\text{soft}}$  and luminosity  $L_{\text{soft}}$ .

Some of the above parameters can be derived almost directly from observations. The electron temperature  $\theta$  of the coronal regions is related to the observed cut-off energy, so that  $E_C \simeq (2 - 3)kT$  (depending on the value of  $\tau$ ). Clearly observations also constrain the slope of the hard X-ray power law and given the temperature and  $\alpha$ ,  $\tau$  is also determined. Furthermore, as it has already been pointed out, the bolometric luminosity of GBHC only changes by small factors despite the dramatic changes in spectral shape. This implies  $L_{\text{soft}} \approx L_{\text{hard}} \approx L_{\text{tot}}$  (where the subscripts 'soft' and 'hard' refer to the soft and hard states).

As we shall see, the other parameters (notably  $T_{\text{soft}}$ ) are related to the system geometry. We associate a temperature to the disk blackbody due to intrinsic dissipation in the disk itself ( $T_{\text{soft}} = 3.8 \times 10^7 [(1-f)/M]^{1/4} (r_{\text{disk}}/50)^{-1/2}$  K). However, we also consider the quasi-thermal emission, due to the re-radiation of the hard X-rays, which is therefore a function of the height of the active regions. Flares triggered close to the disk would heat up small areas of the accretion disk (small covering factor), but contribute to the hottest blackbody emission. On the contrary, flares at large vertical scales irradiate much larger areas but the locally re-processed energy density is small compared to the intrinsic dissipated flux and thus do not affect  $T_{\text{soft}}$ .

In order to give a simple description of such geometrical effects we schematically represent the active regions as spherical volumes of typical scale (radius)  $r$ , distributed at different scale heights  $h$  above the (geometrically thin) disk, and extending over an area out to a radius  $r_{\text{disk}} \approx 50$ . Where  $r$ ,  $r_{\text{disk}}$ ,  $h$  and  $R_{\text{hot}}$  (see below) are all in units of Schwarzschild radius,  $R_S = 2GM/c^2$ .

If we then assume that half of the luminosity from each dissipation region is directly detectable, then the amount of flux per solid angle going back and impinging onto an area of radius  $R_{\text{hot}}$  of the disk is given by

$$F(R_{\text{hot}})dR_{\text{hot}} = \frac{L}{4} \frac{h}{(R_{\text{hot}}^2 + h^2)^{3/2}} dR_{\text{hot}} \quad (2)$$

where  $L = L_{\text{tot}}/N$  is the luminosity of one active region. The re-radiated flux from this same area (in a steady situation) corresponds to  $\sigma T_{\text{hot}}^4 = F(R_{\text{hot}})$ . For a given height  $h$ , we define a typical relevant radius  $R_{\text{hot}}$  as the radius at which the temperature has decreased by a factor  $\sim 2$ . This corresponds to  $R_{\text{hot}} \approx 2.3h$  (or approximately  $= 2.3h + r$  for small  $h$ ).

Consistently, the soft photon field from the disk might be amplified in those areas, of radius  $R_{\text{hot}}$ , located below the active regions and even dominate over the intrinsic cyclo-synchrotron radiation. This is more likely to happen in those regions close to the accretion disk itself (small  $h/r$ ).

This is the key feature of the model: the active coronal regions play a crucial role in the production of both the hard power-law and the hot blackbody components observed in the X-ray spectra of GBHC.

The hot blackbody emission visible in the soft state is the result of the heating, and consequent re-radiation of the hard X-rays produced by those magnetic flares triggered at low  $h$ . The hard power-law tail in the soft state (and in the

hard state if the active regions are large enough), is due to inverse Compton scattering of the soft disk photons by the high energy electrons. In the hard state however, the hard power-law component is usually due to inverse Compton of the photons produced as thermal cyclo-synchrotron radiation. From the above discussion, it is then apparent that the only free parameters in this scenario are the typical scales, height  $h$  and dimension  $r$ , of the flares above the disk.

In the next two sections we shall directly investigate the spectral implications of having flares at different heights  $h$  by comparing the model predictions with the observations of GX339-4.

### 3 THE GX339-4 DATA

GX339-4 shows a wide range of energy spectral shapes and variability patterns, allowing it to be classified as being in the off, low, intermediate, high, or very high states. In order to examine these different states we have considered the observations available in the literature on the full-band spectra, which covered as many states as possible. Here we review the data for each one of the spectral states of GX339-4, which will be represented by their spectral model fits in our figures. These are not intended to represent any realistic physical model but merely provide a way of describing the data.

#### 3.1 Soft/High State

Observations of GX339-4 in its soft state have been reported by Makishima et al. (1986). The object was observed simultaneously in the X-ray and optical bands, using the X-ray satellite *Tenma* (2–20 keV) and the Anglo Australian Telescope, respectively. The X-ray spectrum comprises a very soft component modeled with a disk-blackbody at a temperature of 0.7 keV and a hard tail represented by a power law. We have selected two of the reported observations which show an increase in the intensity of the hard tail (the soft X-ray component is always very stable). Observations by Ariel-6 (2–10 keV) of this soft component are also presented by Ricketts (1983) and the spectrum is described with a power law of photon index  $\Gamma = 4.5$ . GX339-4 was observed by the HEAO 1 (12–200 keV) satellite (Nolan et al. 1982) and these data, also, showed these two spectral components. The two observations, fall 1977 and spring 1978, were fitted using model functions which are the sum of a power law and bremsstrahlung emission.

At higher energies, the hard tail of GX339-4 has been observed by BATSE (20-300 keV; Harmon 1994) and SIGMA (35-1300 keV; Bouchet et al. 1993). In 1991 both instruments simultaneously observed the source during an outburst making a transition from the hard to the soft state. All the spectra can be well represented by a thermal bremsstrahlung model ( $kT \sim 100$  keV).

*Optical data:* Doxey et al. (1979) and Motch, Ilovaisky & Chevalier (1985) observed the object in May–June 1978 and Feb–Mar 1982, respectively; its magnitude was reported to be  $V=16.6-16.7$ , similar to the AAT observation ( $V=16.5$ ) reported by Makishima et al. (1986).

As already mentioned, in the soft X-ray state the source

does not show either optical or X-ray short time scale variability.

#### 3.2 Very High State

GX339-4 was observed with *Ginga* (4–28 keV) in its very high state (Miyamoto et al. 1991), with a spectrum similar to the hard state, consisting of a low energy component (disk blackbody at  $kT \sim 1$  keV) and high energy tail (power-law with  $\Gamma = 2.5$ ). The X-ray intensity was a factor 2-3 larger than in the high/soft state, but unexpectedly showed very rapid variations on time scales of less than several minutes in the power law tail.

#### 3.3 Intermediate State

Data from the EXOSAT ME (1–20 keV) has revealed the presence of an intermediate state, characterized by a soft spectral component (fitted by a blackbody with  $kT = 0.42$  keV) and a relatively steep, harder power-law tail ( $\Gamma = 3.5$ ; Mendez & van der Klis 1997).

#### 3.4 Hard/low State

GX339-4 was observed in its hard state on a few occasions with *Ginga* in Nov 1991 (Ueda, Ebisawa & Done 1994). In all cases the energy spectra were well represented by a single power law component with a typical photon index of  $\Gamma \sim 1.7$ . Ariel-6 observations (May 1981) found the source in its hard state with a spectral slope of  $\Gamma = 1.5$  in the 1–20 keV band (Ricketts 1983; Motch et al. 1983).

The high energy X-ray spectrometer on board of OSO 8 observed GX339-4 in Sep 1976. Dolan et al. (1987) fitted the hard state spectrum with a power law with  $\Gamma \sim 2$  in the 16–151 keV energy range. BATSE observed GX339-4 in its low state in Jul–Sep 1991 (Harmon et al. 1994) and the 20–300 keV spectrum during this outburst was fitted by a bremsstrahlung model ( $kT \sim 100$  keV for the July observation and  $kT \sim 60$  keV at the end of the outburst in September). Simultaneous OSSE (59–400 keV) and SIGMA (35–1300 keV) data (Sep 1991) were reported by Bouchet et al. (1991) and Grabelsky et al. (1995), respectively. We include bremsstrahlung fits to these data also.

*Optical data:* The Ariel-observations (May 1981) were simultaneous with optical fast photometry (Motch et al. 1981; Motch et al. 1983). During this period the optical counterpart was reported to be extremely bright, with  $V=15.4$ . More remarkably, the optical flux showed very short time scale activity (flares as short as 10–20 ms during which the flux increased by a factor up to 5; Motch et al. 1983). The source also appeared to be redder in the infrared band during the May 1981 activity phase (Motch et al. 1982).

Note that short timescale variability has consistently been observed when the object is in its hard state.

#### 3.5 Off state

Ueda et al. (1994) reported on observations with *GINGA* from 1989 to 1991. The 1989 data were also (see above) well represented by a power law ( $\Gamma \sim 1.7$ ) but with much lower intensity than in 1991. During the off state observed

by EXOSAT in Apr 1985 the source was found to exhibit a hard power law spectrum ( $\Gamma = 1.8$ ; Ilovaisky et al. 1986). The spectrum of the off state was also recorded in Sep 1988 by HEXE (30 – 180 keV) and fitted with a power law of 2.2 (Dobereiner et al. 1989).

In its off state the optical counterpart of GX339-4 becomes exceptionally faint,  $V \gtrsim 18$  (Motch et al. 1983).

#### 4 APPLICATION TO GX339-4

We can now compare more specifically the model predictions against the data available for GX339-4.

We recall that the main parameters that allow us to describe the spectrum are determined by our choice of geometry, i.e.  $(h, r)$ . The blackbody emission is calculated self-consistently for a given height: the intrinsic energy dissipation in the accretion disk gives  $T_{\text{soft}}$ ; the re-radiation of the hard X-rays determines the effective temperature  $T_{\text{hot}}$  in those areas, of dimension  $R_{\text{hot}}$ , of the disk heated by the active regions.

In the regime considered, the cyclo-synchrotron emission is self-absorbed\*. The soft photons (both in the effective blackbody component and in the cyclo synchrotron peak) are Comptonized in the active regions.

It should be stressed that, as our purpose is to determine any constraint on the global properties of the active regions, there is no attempt to perform actual best fits to the data, but rather to define the model parameter space consistent with the ‘average’ of different observations for each one of the states.

In the *hard state* of GX339-4 we have  $\theta \simeq 0.18$  (derived from the spectral cut-off in the data) and  $\alpha \approx 0.4 - 0.5$  (considering several observations) which imply  $\tau = 1.35$ . The soft component is not observed in this state; this immediately implies that flares are unable to heat up the intrinsic blackbody disk emission (which peaks in the UV – see Fig. 1) because they are either intrinsically weak or located high above the disk. As we shall discuss later, the power released in a single flare is constrained to be quite high, and therefore we can only reproduce the hard state assuming that  $h \approx 3.3$ , i.e.  $\sim 10^7$  cm for a  $10 M_{\odot}$  black hole.

Depending on the dimension of the active regions, the high energy component is dominated by Comptonization of either internal cyclo-synchrotron photons or blackbody ones. This implies that  $r$  is not tightly constrained by observations, and can range between  $0.05 - 3.3 R_{\text{S}}$ : in compact (i.e. high  $B$ ) regions the intrinsic cyclo-synchrotron soft photon field dominates (Fig. 1b), while for larger  $r$ , the photon energy density is dominated by the soft disk photons (Fig. 1a).

Note that the two different Comptonized power-law components are renormalised according to the relative timescales associated with the corresponding radiative processes. This implies that, although in some cases the cyclo-synchrotron emission does not contribute significantly to the observed spectrum, it still influences the normalization of the component due to inverse Compton on soft disk photons.

\* The formalism used to determine the self-absorbed frequency is described in Di Matteo et al. (1997).

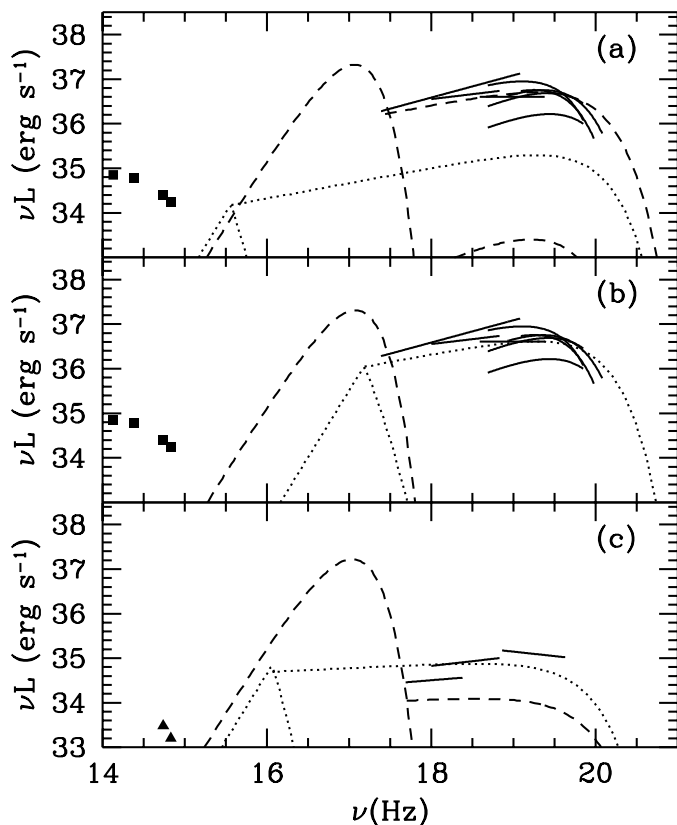


**Figure 1.** Representative model predictions (dotted and dashed lines) plotted against fits to the data (represented by the solid lines) for the *hard state* (a and b) and *off state* (c) of GX339-4. The flares are triggered high above the disk so that their emission does not affect the intrinsic temperature of the accretion disk, whose blackbody emission is represented by the dashed line. (a) The spectrum results from the intrinsic blackbody emission from the accretion disk and its Comptonization, for  $\tau = 1.35$ ,  $\theta = 0.18$ ,  $r = 2$  and  $h = 3.3$ . (b) The hard X-rays are dominated by Comptonization of soft seed photons originating as thermal cyclo-synchrotron radiation in the active region (dotted lines).  $\theta$ ,  $\tau$  and  $h$  are the same as in case (a). The dimension of the active regions is instead  $r = 0.1$ . (c) In the *off state* the parameters are the same as those for the hard state of case (b) apart from  $\theta$  which is in this case 0.13. The data (solid lines) are those described in sections (3.4) and (3.5).

The *off-state* can be ‘fitted’ with very similar parameters,  $h = 3.3$ ,  $r = 0.3 - 1$  and a slightly lower electron temperature,  $\theta = 0.13$  (the data do not provide a clear indication of a spectral cut-off in this state). Even a small decrease in the electron temperature implies much less cyclo-synchrotron emission (Fig. 1c), requiring  $r$  to be adjusted quite finely in order to account for the Comptonized hard X-ray spectrum.

The emission in the *soft state* is dominated by the soft thermal component. Within the context of our model this hotter quasi-blackbody component can be generated by the hard X-ray radiation impinging onto and being reprocessed in the disk. When flares are triggered close enough to the disk, namely at  $h = 0.1$ , i.e.  $\sim 3 \times 10^5$  cm, the temperature in the areas of radius  $R_{\text{hot}}$  achieves the observationally required values to explain the  $\approx 1$  keV blackbody emission. Note that, if the dissipation in magnetic flares is compara-

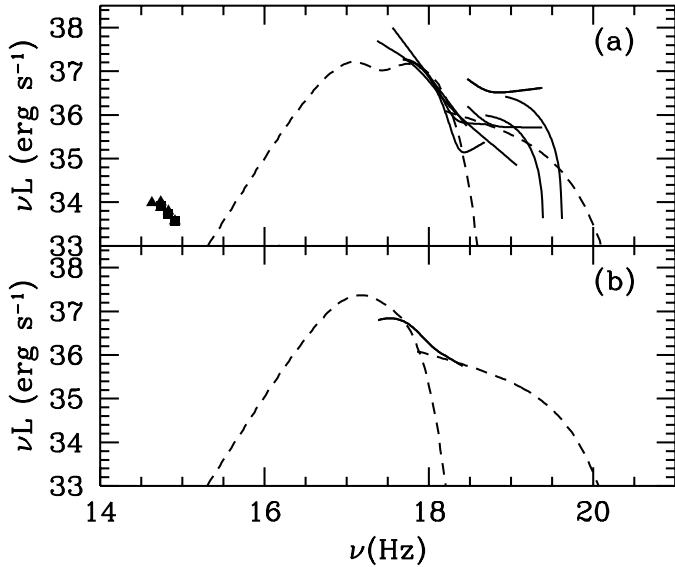


**Figure 2.** Model predictions (dashed lines) plotted against fits to the data (solid lines) for the (a) *soft state*, and (b) *intermediate state* of GX339-4. The temperature in the disk areas of radius  $R$  heated by the flares increases, giving rise to the hotter blackbody component. The power-law component is due to Comptonization of these same blackbody photons. (a)  $\theta = 0.08$  and  $\tau = 1.35$ . The dimension of the active regions is  $r = 0.4$  and its height above the disk is roughly equivalent to its dimension,  $h = 0.1$ . (b)  $\theta = 0.08$ ,  $\tau = 1.35$  (as before)  $h = 2$  and  $r = 1$ . The data are those described in sections (3.1) and (3.2).

ble in the hard and soft states, this mechanism naturally accounts for the similar luminosity observed in the two states. Fig. 2 shows this additional blackbody component due to flare reradiation.

The energy of the spectral cut-off implies electron temperatures lower than in the hard state, i.e.  $\theta = 0.08$ , and by imposing  $\alpha \approx 1.5$ , the optical depth  $\tau = 1.35$  is consistent with being constant between the two main spectral states.

The dimension of the active region is constrained in a rather small interval,  $r = 1 - 4$ , overlapping with the upper range of that of the hard state case. Because of the lower  $\theta$ , the self-absorbed cyclo-synchrotron emission ( $\nu L_\nu(\text{synchro}) \propto \theta^7$ ) cannot significantly contribute to the seed photons field for the hard tail, which is instead due to inverse Compton of soft disk photons (Fig. 2a).

The *intermediate state* is also dominated by the blackbody component but this is at slightly lower temperatures than in the soft state. Within our model, this most naturally arises from flares at intermediate heights, with  $h \sim 2$  and  $r \sim 1$  (Fig. 2b). Finally, in the *very high state* the blackbody component of GX 339-4 is similar to that observed during the soft state but the normalization of the power-law tail is higher. This can be easily explained by a larger covering fraction ( $r \sim$  a few) of the active regions.

In summary, the hard state requires parameters of the active regions quite similar to those of the soft state. The two primary differences are to do with the fact that in the soft state active regions are mostly at small  $h$  and have lower electron temperature  $\theta$ , whereas in the hard state are characterised by higher  $h$  and  $\theta$ . All the other states can easily result from intermediate values of these parameters.

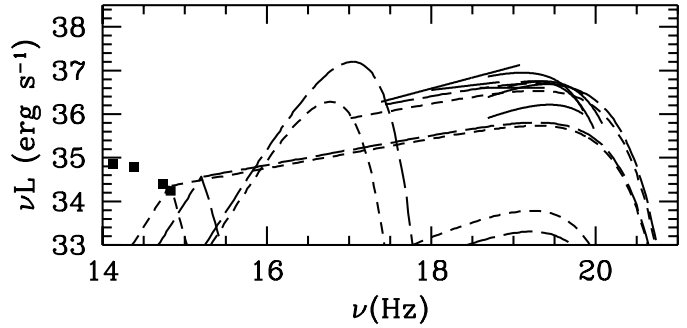


**Figure 3.** The cyclo-synchrotron emission peaks in the optical for either  $f = 0.9$ ,  $N = 100$  and  $r = 3$  (short dashed lines), or  $f = 0.8$ ,  $N = 100$ ,  $r = 1.3$  (long dashed lines).  $h$ ,  $\theta$  and  $\tau$  are the same as in Fig. 1b. This can explain the short timescale optical variability detected in the observations by Motch et al. (1983—filled squares).

In other words, the heart of this model is the choice of the geometry. Depending on whether the flares are high above the disk or close to it the spectrum changes from being hard to soft respectively (and therefore gives rise to the hard state or the soft). When the flares are located high above the disk (and they are few in number), the solid angle they subtend to the soft photon field produced in the disk is small: the system is photon starved and the Comptonized spectrum hard, as required by observations (synchrotron radiation is highly self-absorbed and therefore its Comptonization highly saturated also). A photon-starved system can naturally account for the spectral characteristics of the hard state. Conversely, when a large number of flares is triggered very close to the disk surface, the soft photon field is highly enhanced giving rise to a hotter blackbody component (due to reprocessing in the disk itself) and a very soft Comptonization spectrum.

Before concluding this section we would like to point out an interesting feature of our model. This concerns the role of the cyclo-synchrotron emission. If the number of active regions increases to  $N = 50 - 100$ , the cyclo-synchrotron emission peaks at much lower frequencies and can explain the observed optical flux, as shown in Fig. 3. An increase in  $N$ , in fact, corresponds to a decrease in the intrinsic magnetic energy released in each loop. If this occurs, then variations in optical flux are expected to occur on short timescales (related to the size of our active regions, as indeed observed by Motch et al. (1983) in GX339-4. This increase in covering fraction can also explain the anti-correlation between optical and X-ray variations (Motch et al. 1983). As we see in Fig 3, when the optical emission is due to the intrinsic synchrotron emission (and variations in the optical are expected) the X-rays are produced by Comptonization of the external soft blackbody radiation (see Fig 3). As already discussed, when this process dominates the dimension of the active regions needs to be increased, implying a much larger covering fraction (with  $N = 100$ ), and therefore much slower variations in the X-rays with respect to the standard hard state in Fig 1.

#### 4.1 Other model parameters

It is important to stress that the value of the other model parameters (notably  $N, f$ ) does not need to be tuned finely. Let us consider them in turn.

In the hard state, an increase in number of the active regions implies a (slow) decrease in  $B$ . If  $N = 10 - 50$  the Comptonization on cyclo-synchrotron photons still dominates, but as  $N$  reaches  $\sim 100$  (see also Fig. 3), this component decreases significantly (as  $B$  does). This implies that the dimension of each region needs to be increased for Comptonization of the external photons to account for the observed flux.

In the soft state case, the most relevant modification is the amount of flux dissipated in each region, which in turn affects the effective temperature  $T_{\text{hot}}$  which decreases as  $N$  increases (the active regions are more numerous but less powerful and thus do not heat significantly the underlying disk). For  $N \gtrsim 50$  the soft blackbody component (due to re-radiation) becomes too cool to explain observations.

On the other hand, the power magnetically dissipated, i.e.  $f$ , might be lower. This implies that the normalization of the disk blackbody component increases but, even for  $f = 0.2$ , the dominant radiative contribution in the hard state is still from cyclo-synchrotron emission and its Comptonization. In the soft state instead the net effect is a change in the relative normalizations of the two blackbody components.

#### 4.2 Statistical fluctuations?

We have shown that all of the different states can be obtained with appropriate choices of  $\theta$  and  $h$ . Clearly the fundamental point is to interpret these findings in a coherent and self-consistent physical picture of the whole process and in particular of the change of the spectral states of the source.

However, before dealing with this point, a key question which needs answering is whether the spectral information requires that in each state the dissipating coronal region is pervaded only by active regions with given characteristics or is consistent with a spectral state dominating over another although ‘different’ active regions are present at the same time. In other words, we examine whether it is possible to have  $N = 10$  active regions associated with one particular temperature and  $h$  and say  $N = 7$  (a statistical fluctuation on  $N$ ) flares at different  $h$  and  $\theta$ , but still have the ‘main’ state dominating.

We find that statistical fluctuations are inconsistent with observing any one particular spectral state. More precisely, in order to have the hard state, we can only have active regions at  $h = 3.3$  and no regions (within a random fluctuation) at lower  $h$  can be active simultaneously. The temperature instead is not constrained, so that at each height  $h$  regions can have different temperatures (ranging from  $\theta = 0.08$  – soft state to  $\theta = 0.18$  – hard state). The predicted spectrum in the soft state is inconsistent with random fluctuations for both regions at different heights and at different temperatures.

### 5 THE PHYSICAL PICTURE

In this section we discuss how the geometric representation adopted for the different states relates to the physical picture in which coronal loops, emerging from the disk by magnetic buoyancy, reconnect and dissipate their energy in powerful X-ray flares.

#### 5.1 Magnetic buoyancy and reconnection

From the comparison of the model predictions with the observations of GX339-4 we find that, in order to reproduce the different spectral states, the active regions have to be located at different heights above the accretion disk with temperatures inversely proportional to their height. This anti-correlation is indeed (qualitatively) expected in the physical frame of reconnection driven by magnetic buoyancy.

Let us briefly recall the general picture associated with a magnetically structured corona. Strong fields in the accretion disk are continuously generated because of the shearing and the turbulent disk flow serves as an effective dynamo that can rapidly strengthen a seed field. Because intense fields are strongly buoyant they rapidly emerge from the disk thereby releasing part of the accretion energy into a corona in the form of magnetic energy. This disk instability is therefore (qualitatively) equivalent to flux emergence on the Sun as originally discussed by Galeev, Rosner & Vaiana (1979). As the instability develops, the gas slides down the expanding loop, and the evacuated loop rises as a result of the enhanced magnetic buoyancy (the expansion is due to magnetic pressure although the dynamics are controlled by the down flow due to gravity along the rising loop). Consequently, as long as the magnetic pressure at the top of the magnetic loop is larger than the coronal (radiation, gas and magnetic) pressure, the expansion of the loop continues. Magnetic buoyancy of an active region thus naturally decreases the plasma density to the point where the region can efficiently reconnect. In accretion disk coronae this can take place when either a new magnetic flux tube emerges into a pre-existing magnetic configuration or the expansion causes two loops to coalesce; when this happens one expects at least one current sheet to develop.

If it is assumed that steady reconnection is occurring in such a current sheet one can solve the energy equation and therefore determine the temperature of the plasma as a function of the height of the current sheet in the corona. From this type of analysis it has been found that, if the sheet rises to a certain height, there will be no neighbouring equilibrium situation, implying a sudden increase in temperature (eg. Heyvaerts, Priest & Rust 1977, Shibata et al. 1989 and references therein). Joule heating can no longer be balanced by radiation and so the sheet heats up explosively. The sheet will then try to achieve a stage where Joule heating can be balanced by thermal conduction or radiative cooling. At this point, the current sheet achieves the critical temperature for the onset of turbulence (creation of a slow shock), with the result that the flare is triggered. This is the main phase of the flare, the current sheet reaches a new steady state, with reconnection based on a marginally turbulent resistivity (anomalous resistivity) and X-ray flares being the after effect of the energy release by the slow shocks (e.g. Di Matteo 1998). The geometry which we have described

here is broadly consistent with the above picture. In fact, in the soft state the magnetic loops do not rise high above the accretion disk and the temperature for the onset of reconnection is expected to be lower. Current sheets high above the accretion disk, as required for the hard spectral state, would instead have reached higher temperatures by the time flares (fast reconnection) are triggered.

## 5.2 The two states: different phases of magnetic field dissipation?

We would now like to incorporate the geometrical description of the different states with an understanding of the physical reasons which regulate the selection of the different scale heights for the magnetic flares. In the physical context of buoyancy and reconnection, this implies investigating the reasons why magnetic flux tubes, in the soft state, are unable to buoyantly expand and grow higher into the corona before reconnecting and triggering X-ray flares and conversely why magnetic buoyancy can be much more effective at selecting higher scale heights in the hard state.

Let us assume that the rate of magnetic energy dissipation is constant and the key difference in the two states originates from the way this energy is released into the corona. As already mentioned, magnetic buoyancy instability would take place in those regions of the disk where shear stresses acting on the a flux tube generate a magnetic pressure which becomes comparable with (and eventually exceeds) the disk gas pressure. The gas pressure inside a standard (thin)  $\alpha$ -disk at a distance of  $r_{\text{disk}} \simeq 50$  is of the order of  $P_{\text{gas}} \sim 2 \times 10^{12} \text{ erg cm}^{-3}$  (a viscosity parameters  $\alpha_v \sim 10^{-2}$  has been assumed). Magnetic field building up in such a disk will then become buoyant in those regions where  $\beta = P_{\text{gas}}/P_{\text{mag}} \approx 1$ , i.e. where it reaches a strength  $B \sim 6 \times 10^6 \text{ G}$ . Magnetic loops from these regions will eventually emerge into the coronal regions but their expansion could be halted as soon as they enter it for reason which we explain below. If  $B$  in each magnetic loop is set from the buoyancy instability (as derived above) and the available magnetic energy is some fraction of the accretion power as set by eqn. (1) we deduce that the total number of magnetic loops emerging from the disk at any time can be of the order of  $N_{\text{tot}} = 10^2 - 10^3$ . In a very simplified picture we can then assume that reconnection takes place every time two such loops touch each other. We simulate about  $10^3$  loops of radius  $r = 0.3$  (see soft state in Fig. 2) in random positions on the surface of an accretion disk of radius  $r_{\text{disk}} = 50$  and find that at any given time there will be about 10 loops interacting with each other by the time they reach  $h \sim 0.3$ . This constitutes the number of regions  $N$  that we have required to be active at any time in the soft spectral state (consistently, if there are  $N \sim 10$  active regions and the timescale for upward buoyancy forces to remove the flux tubes from the disk is of the order of  $\Omega^{-1} \sim 100 \text{ s}$  (Coroniti 1981, Stella & Rosner 1984), where  $\Omega$  is the Keplerian angular velocity, we expect about  $N_{\text{tot}} \sim 10^3$  flux tubes to emerge from the disk at any given time).

In Section 4 we have shown that, in the hard state, the magnetic field strength (in the loops) needs to achieve higher values in order to explain the observed spectrum. In our scenario, and from the Section 4, this would imply that, in this state, magnetic flux tubes become buoyant when  $B \gtrsim$  a few

$\times 10^7 \text{ G}$ . This, in turn, implies that the same total magnetic energy needs to be released in only  $N \sim 10$  ‘powerful’ loops (see eqn. (1)). These loops rise and expand high above the disk and, according to our simple simulation, would start interacting (a reconnection event would take place) when they reach  $h \approx 3$ . The selection of a small number of higher  $B$  loops, would explain why in the hard state flares can be triggered high above the disk.

In this picture, though, it is hard to identify the mechanism that leads to a change in the spectral states. In other words, it is not clear why the system would lock up in a certain state and what physical conditions would cause the transition to another state in the relevant timescales. It is interesting to note, though, that the magnetic field energy density in the powerful loops in the hard state ( $B \sim 10^7 \text{ G}$ ) is in equipartition with the radiation pressure provided by the active flaring close to the disk during the soft state ( $P_{\text{rad}} \sim 3 \times 10^{14} \text{ erg cm}^{-3} > P_{\text{gas}}$ ). This suggest that the strong radiation pressure impinging on the disk may be forcing the magnetic field, in the buoyantly unstable loops, to grow to larger values in order to be able to rise in the coronal atmosphere. In other words, we expect that such an intense flare activity so close to disk, would modify the physical condition of the disk itself (or at least affect the top layer of the disk).

It is also worth noticing that, according to the picture we have described above, in both states the magnetic field strength, when loops reconnect and reach their respective maximum heights, is similar to the external coronal radiation pressure. It is not clear how the magnetic field interacts with radiation (either in the corona, or in the radiation dominated part of the disk) but it seems intriguing that in the Soft state case, flares are triggered close to the disk and the ambient radiation pressure (due to intrinsic blackbody emission in accretion disk) is of the order  $P_{\text{rad}} \approx 10^{12} \text{ erg cm}^{-3}$  in the corona ( $B \sim 6 \times 10^6 \text{ G}$  in the loops). In the hard state the loops expand as to reach  $h \sim 3$  which implies that the magnetic pressure at the top of the expanding loops ( $B \propto h^{-1}$ ; Shibata et al. 1989) becomes comparable to the ambient coronal radiative pressure ( $P_{\text{rad}} \sim 3 \times 10^{11} \text{ erg cm}^{-3}$ ). We speculate therefore that the loops expansion might be halted when the internal magnetic pressure equalizes the ambient radiation (total) pressure in the corona. Because of the intrinsically lower  $B$  field (see above) in the soft state magnetic loops would be strongly decelerated as soon as they enter the corona which explains why no large (high  $h$ ) loops would be present in this state.

This (admittedly qualitative) picture has some intriguing features, most notably it accounts for the a priori unpredictable physical properties required by the spectral observations under reasonable assumptions.

## 6 VARIABILITY AND REFLECTION

At least two major observed features need to be accounted for in a consistent description of the change in spectral states of GBHC, namely variability and the properties of X-ray reflection features.

In the model discussed above, the extremely rapid and intense variability on the high energy component observed during hard states fit well into the picture. In the situa-



tion described above in fact, during this phase only a few powerful loops would be present at any time. Any reconnection event would then produce a significant flux change and the typical timescale for the formation of a new structure would probably occur in a detectable timescale of the order of  $hR_S/c \sim$  ms. On the contrary the numerous potentially active region in the soft state would individually be associated with smaller flux dissipation, occurring over a timescale  $\sim 10 \mu\text{s}$ , i.e. the variability would result in flickering not currently detectable.

X-rays impinging on the disk are also expected to be reflected with different spectral properties in the two states. While in our situation the covering factor is of the order of 0.5, the ionization state of the illuminated disk would be strongly different. In the hard state, ionization parameters  $\xi \gtrsim 10^2$  can be inferred over most of the disk area. In the soft state,  $\xi \simeq 10^3$  over the majority of the disk and  $\xi \gg 10^4$  over 10 per cent of it. As mentioned earlier, GBHCs in the hard state have similar spectra as Seyfert galaxies but with a much less prominent reflection component. In the hard state, a ionization parameter  $\xi \gtrsim 10^2$ , is in broad agreement reflection parameters deduced from observations. Detailed models of reflection for highly ionized disks would need to be developed in order to make specific predictions for the reflection features in the hard states of GBHCs.

Nayakshin & Melia (1997b) have shown that the differences in the spectrum, in the ionization state of the cold disk and in the iron lines and edges in the hard state of Cyg X-1 compared to the observed Seyfert galaxies may be a natural consequence of a change in the physical state of the 'transition layer' where the hard X-rays from the active regions are reflected or reprocessed. They also argue that if X-rays are emitted by localized magnetic flares above the cold accretion disk, then the energy deposited by the X-rays cannot be reradiated fast enough to maintain equilibrium, unless the X-ray skin heats up to the Compton temperature, at which point the gas is mostly ionized. As a result, most of the incident X-rays are Compton reflected back into the active region before reaching the cooler disk where the reprocessing occurs so that the amount of cooling due to the soft radiation re-entering the active region is drastically reduced.

## 7 DISCUSSION

We have discussed the implications on the spectral states observed in GBHC of a magnetically-structured corona model, in which magnetic flares may result from reconnection of flux tubes rising above the cold accretion disk due to magnetic buoyancy. Using a simple geometrical representation which takes into account the scaling of the different quantities with height of the corona above the disk, we have shown that the hard X-ray state in GBHC can be produced by flares located high above the underlying disk via Comptonization of either the cyclo-synchrotron radiation or the photons produced in the disk. The soft state is instead due to flaring of active regions close to it. The soft blackbody component is in this case dominated by the re-radiated X-ray field and the hard tail is produced via Comptonization of this same soft radiation. Depending on whether the flares are high above the disk or close to it the spectrum changes from being hard to

soft respectively (and therefore gives rise to the hard state or the soft). When flares are triggered high above the disk the system is highly photon starved and therefore the Comptonized spectrum very hard. Conversely when a large numbers of flares are triggered very close to the disk the soft photon field is highly enhanced; this naturally accounts for the a hotter blackbody component (due to reprocessing in the disk itself) and the very soft Comptonization spectrum typical of the soft state. By varying the typical scale height and scale size of the dissipative regions, the spectra for all of the five states observed in GX339-4 can be qualitatively reproduced. Applying the model to GX339-4 has allowed us to determine constraints both on the geometrical and physical properties of such active regions.

We have qualitatively integrated the geometrical description of the different states in the physical context of magnetic buoyancy. We have shown that in the soft state, buoyancy instability in an accretion disk (which only dissipates a small fraction of the total energy) naturally favors the emergence of possibly a large number of relatively weak magnetic field flux tubes (maybe when the dynamo action is initiated in the disk). Because such tubes have a low internal pressure their expansion is basically halted as soon as they enter the coronal regions. This is the reason why the flaring occurs really close to the accretion disk itself. Conversely, the hard state could be due to a typically different phase of magnetic energy dissipation (maybe as the dynamo action builds higher magnetic fields). This would take place in a small number of very intense magnetic field loops. The reason why flares would reach higher scale heights, in this model, can then be ascribed to the intrinsically more intense magnetic field loops which would lead the loops to grow and expand before efficient reconnection takes place. Also, large loops would naturally form from small scale ones. Reconnection between small loops can drive a time-dependent inverse cascade process which leads to the formation of larger structures and cause spectral changes.

While the model described is certainly too schematic both in its geometrical/uniformity and physical assumptions it seems to account qualitatively for other observed properties of GBHC, namely the variability and characteristics of the reflected X-ray component.

In other models proposed to account for the spectral states of black hole candidates the amount of power dissipated in the accretion disc varies greatly from one state to the other, so that it is almost negligible in the hard state while dominating in the soft one. The model examined here on the contrary postulates that a constant fraction of the total power is radiatively dissipated in the disk. Most of the energy is instead released in magnetic coronal flares at different heights above the disk. The amount of heating and re-radiation from the accretion disk itself during the triggering of flares can naturally give rise to all of the spectral components observed in the different states of the source.

## 8 ACKNOWLEDGMENTS

Trinity College (TDM), the Italian MURST and IOA (PPARC theory grant) (AC) and the Royal Society (ACF) are thanked for financial support.

## REFERENCES

- Bouchet L., 1993, *ApJ*, 407, 739  
 Coroniti F.V., 1981, 244, 187  
 Di Matteo, 1998, submitted  
 Di Matteo T., Celotti A., Fabian A.C., 1997, *MNRAS*, 291, 805  
 Dolan J.F., Crannel C.J., Dennis B.R., Orwing L.E., 1987, *ApJ*, 322, 324  
 Dobereiner S. et al. 1989, Proc. 23rd ESLAB Symp on two Topics  
 In X-ray Astronomy, Bologna, Italy (ESA SP-296)  
 Dove J.B., Wilms J., Maisack M., begelman M.C., 1997, *ApJ*, 487, 579  
 Doxey R., Grindlay J., Griffiths R., Bradt H., Johnston M., Leach R., Schwartz D., Schwartz J., 1979, *ApJ*, 228, L67  
 Esin A., McClintock J.E., Narayan R. 1997, *ApJ*, 489, 865  
 Galeev A.A., Rosner R., Vaiana G.S., 1979, *ApJ*, 229, 318  
 Gierlinski M., Zdziarski A., Done C., Johnson, W.N., Ebisawa K., Ueda Y., Haardt F., Phlips B., 1997, *MNRAS*, 288, 958  
 Grabelsky D.A., Matz S.M., Purcell W.R., Ulmer M.P., Grove J.E., Johnson W.N., Kinzer L.D., Kurfess J.D., Strickman M.S., Jung G.V., 1995, *ApJ*, 441, 800  
 Haardt F., Maraschi L., Ghisellini G., 1994, *ApJL*, 432, L92  
 Harmon B. A., et al. 1994, *ApJ*, 425, L17  
 Heyvaerts J., Priest E.R., Rust D.M., 1977, *ApJ*, 216, 123  
 Ilovaisky S.A., Chevalier C., Motch C., Chiappetti L., 1986, *A&A*, 164, 67  
 Makishima K., Maejima Y., Mitsuda K., Bradt H.V., Remillard R.A., Tuohy I.R., Hoshi R., and Ankagawa M., 1986, 308  
 Mendez M., van der Klis, 1997, *ApJ*, 479, 926  
 Motch C., Ricketts M.J., Page C.G., Ilovaisky S.A., Chevalier C., 1983, *A&A*, 119, 171  
 Motch C., Ilovaisky S.A., Chevalier C., 1985, *Space Science Reviews*, 40, 219  
 Nayakshin S., Melia F., 1997a, 1997, *ApJ*, 490, L13  
 Nayakshin S., Melia F., 1997b submitted to *ApJL*, astro-ph/9709286  
 Nolan P.L., Gruber D.E., Knight F.K., Matteson J.L., Peterson L.E., Levine A.M., Lewin W.H.G., Primini F.A., *ApJ*, 1982, 262, 727  
 Pietrini P., Krolik J.H., 1995, *ApJ*, 447, 526  
 Poutanen J., Krolik J.H., Ryde F., 1998, *MNRAS*, 292, L21  
 Ricketts M. J., 1983, *A&A*, 118, L3  
 Shibata, K., Tajima, T., Steinolfson R.S., & Matsumoto, R., 1989, *ApJ*, 345, 584  
 Stella L., Rosner R., 1984, *ApJ*, 277, 312  
 Stern B.E., Poutanen J., Svensson R., 1995, 449, L13  
 Tanaka Y., Lewin W.H.G., 1995, *X-ray Binaries*, ed. W.H.G. Lewin et al., Cambridge, Cambridge university Press  
 Ueda Y., Ebisawa K., Done C., 1994, *PASJ*, 46, 107  
 Zdziarski A.A., Fabian A.C., Nandra K., Celotti A., Rees M.J., Done C., Coppi P.S., Madejski G.M., 1994, *MNRAS*, 269, L55  
 Zdziarski A.A., Johnson W.N., Poutanen J., Magdziarz P., Gierlinski M., 1997, *Proceedings of 2nd INTEGRAL Workshop*, San Malo, France, p. 373